Available online at www.sciencedirect.com
SCIENCE DIRECT®
Sensors and Actuators B 90 (2003) 82–89
SENSORS AND ACTUATORS B CHEMICAL
www.elsevier.com/locate/sensorb

Production of singlet oxygen by $Ru(dpp(SO_3)_2)_3$ incorporated in polyacrylamide PEBBLES

Maria João Moreno[a,b,*], Eric Monson[a], Ramachandra G. Reddy[c], Alnawaz Rehemtulla[c], Brian D. Ross[c], Martin Philbert[d], Randy J. Schneider[d], Raoul Kopelman[a]

[a]*Department of Chemistry, University of Michigan, Ann Arbor, MI 48109, USA*
[b]*Departamento de Química da Faculdade de Ciências e Tecnologia da Universidade de Coimbra, Largo D. Dinis, 3004-535 Coimbra, Portugal*
[c]*Department of Radiology, School of Medicine, Center of Molecular Imaging, University of Michigan, 1150 W Med. Ctr. Dr., 9303 MSRB 3, Ann Arbor, MI 48109, USA*
[d]*Department of Environmental Health Science, University of Michigan, Ann Arbor, MI 48109, USA*

Abstract

Polyacrylamide (PAA) and amine-functionalized PAA (AFPAA) nanoparticles with disulfonated 4,7-diphenyl-1,10-phenantroline ruthenium ($Ru(dpp(SO_3)_2)_3$) have been prepared. The nanoparticles produced have a hydrodynamic radius of 20–25 nm.

The amount of singlet oxygen ($^1O_2$) produced by $Ru(dpp(SO_3)_2)_3$ as been measured using anthracene-9,10-dipropionic acid (ADPA). A kinetic model for the disappearance of ADPA, by steady state irradiation of $Ru(dpp(SO_3)_2)_3$ at 465 nm, has been developed taking also into account a consumption not mediated by $^1O_2$. This direct consumption of ADPA is evaluated by irradiating in the presence of NaN_3 and is about 30% of the total. All the experimental results are very well described by the model developed, both for free $Ru(dpp(SO_3)_2)_3$ and with this dye incorporated in the nanoparticles.

It is found that the polyacrylamide matrix does not quench the $^1O_2$ produced, allowing it to reach the external solution of the nanoparticles and react with ADPA. When the matrix possesses amine groups, AFPAA, the amount of $^1O_2$ that reacts with ADPA is slightly reduced, 60%, but most of the $^1O_2$ produced can still leave the particles and react with external molecules. The particles produced may therefore be used as sources of $^1O_2$ in photodynamic therapy (PTD) of cancers. The fact that those nanoparticles do not quench significantly the $^1O_2$ makes possible the future development of $^1O_2$ sensors based on PAA nanoparticles with the appropriate sensor molecule enclosed.

Keywords: Photodynamic therapy; Nanoparticles; Singlet oxygen; Ruthenium; Polyacrylamide

1. Introduction

Photodynamic therapy (PTD) is based on the photosensitized production of singlet oxygen by non-toxic dye molecules that penetrate cancer cells [1]. These photodynamic drugs are sometimes delivered using nanoparticles, and ideally are targeted. The singlet oxygen creates other reactive oxygen species (ROS), such as superoxide radicals. These may cause damage to the cell's DNA, lysosomes, mitochondria or membrane, resulting in cell apoptosis, or sometimes necrosis. The main problems are: (i) collateral damage to healthy cells; (ii) limitations on light penetration (beyond a few mm); (iii) cancer cells that develop immunity by pumping drug dyes back out of the cell. In contrast, the photodynamic Probes Encapsulated by Biologically Localized Embedding (PEBBLES) [2] encountered in the present work are designed to target cancer cell membranes, but not to enter the cell or release drugs that enter cells. This avoids back-pumping, as well as protects the drug from being metabolized but, will the singlet oxygen, generated in the PEBBLE, manage to come out of it and attack the cell? Our study addresses this question.

The molecule used in this work for the production of $^1O_2$ 4,7-diphenyl-1,10-phenantroline ruthenium ($Ru(dpp(SO_3)_2)_3$), Fig. 1, presents a high quantum yield of $^1O_2$ production, a high absorption coefficient in the visible spectra and a high photostability, making it an excellent choice for use in PDT. The problem of toxicity of $Ru(dpp(SO_3)_2)_3$ is overcome by

* Corresponding author. Present address: Departamento de Química da FCTUC, Largo D. Dinis, 3004-535 Coimbra, Portugal.
Tel.: +351-962544799; fax: +351-239827703.
E-mail address: mmoreno@ci.uc.pt (M.J. Moreno).

0925-4005/03/$ – see front matter
doi:10.1016/S0925-4005(03)00057-1

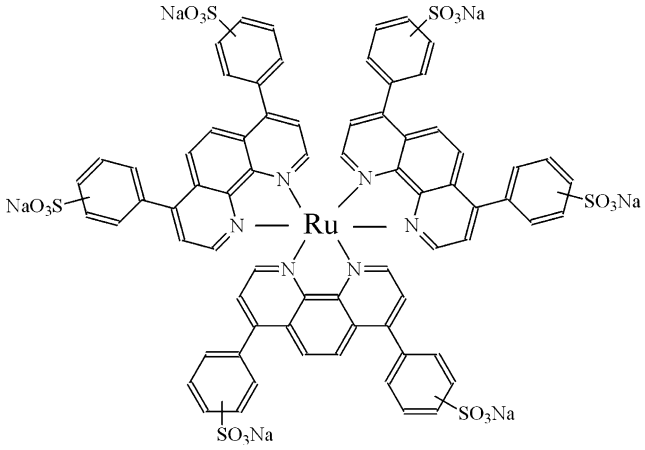

Fig. 1. Structure of the $^1O_2$ source, $Ru(dpp(SO_3)_2)_3$.

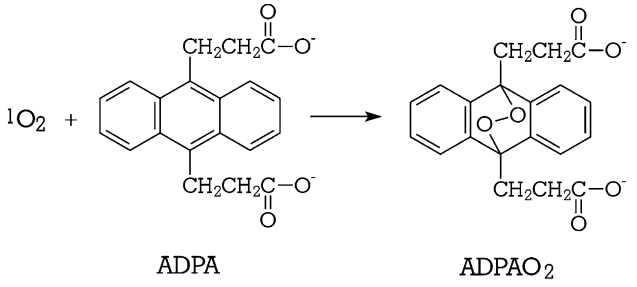

Fig. 2. Reaction of ADPA with $^1O_2$ to form the endoperoxide $ADPAO_2$.

incorporation in non-toxic nanoparticles as seems to be the case for polyacrylamide (PAA) based particles [3,4].

The characterization of $Ru(dpp(SO_3)_2)_3$, free and enclosed in the nanoparticles, as a source of $^1O_2$ was performed with a water soluble anthracene derivative, anthracene-9,10-dipropionic acid (ADPA). This molecule reacts with $^1O_2$ to produce an endoperoxide (Fig. 2). The absorption and fluorescence of the product are benzene-like due to the loss of aromaticity in the central ring and are therefore shifted to the UV (from 400 to 280 nm). This endoperoxide is thermally stable at room temperature [5,6], it is photochemically unstable giving back ADPA [7,8] but at the wavelengths used the endoperoxide does not absorb ($\lambda > 300$ nm). This dye was chosen for the measurement of $^1O_2$ because of its high solubility in water, its high rate constant for reaction with $^1O_2$ [9,10], the thermal stability of the endoperoxide formed and the fact that it does not absorb light at the wavelength used for irradiation of the $^1O_2$ source (465 or 488 nm).

2. Materials and methods

The ruthenium dye $Ru(dpp(SO_3)_2)_3$ was synthesized following the procedure in reference [11]. All reagents and solvents were analytical or chromatographic grade and were purchased from Sigma–Aldrich (Milwaukee, WI, USA) or Polysciences Inc. (Warrington, PA, USA). Fluorescent dyes were purchased from Molecular Probes (Eugene, OR, USA).

The nanoparticles were prepared by polymerization in reverse micro-emulsion as described in [2] with some minor changes. The polymerization solution of PAA nanoparticles consisted of 10 mM phosphate buffer, pH 7.4, with 21% (w/v) of acrylamide, 6% (w/v) of *N*,*N*-methylenebis(acrylamide) and 0.5–5 mM of $Ru(dpp(SO_3)_2)_3$. For the amine-functionalized PAA (AFPAA) nanoparticles 4% (w/v) of *N*-(3-aminopropyl)methacrylamide was used and the concentration of acrylamide was reduced to 17% (w/v). Two milliliters of the above aqueous solution was added to 43 ml of de-oxygenated hexane containing 3.6 mmol of AOT and 8.1 mmol of Brij 30. The polymerization was initiated by the addition of 30 (40) μl of a solution of 10% (w/v) ammonium persulfate in water and 15 (30) ml of *N*,*N*,*N*′,*N*′-tetramethylethylenediamine (TEMED) for the PAA (AFPAA) nanoparticles.

The size of the PAA nanoparticles was measured using multi-angle light scattering with a previous size separation using AFFF—asymmetric field flow fractionation from Wyatt Technologies (Santa Barbara, CA, USA). The solvent used to dissolve the sample and to perform the fractionation was phosphate buffer 10 mM, pH 7, with 0.15 M of NaCl.

UV-Vis absorption was performed in a Shimadzu UV160U (Shimadzu Scientific Instruments, Columbia, MD, USA) and the fluorescence measurements in a FluoroMax-2 spectrofluorometer (ISA Jobin Yvon-Spex, Edison, NJ, USA). In a typical experiments for $^1O_2$ production/measurement 2.5 ml of the $Ru(dpp(SO_3)_2)_3$ solution in phosphate buffer 10 mM, pH 7–7.4, with 0.15 M NaCl, and 12 μM of ADPA was placed in a cuvette with mixing using a magnetic stirring bar. The fluorescence emission of ADPA when excited at 380 nm was recorded and the solution was then irradiated at 465 nm, with a bandwidth of 10 mm, for 3 min. The measurement of ADPA fluorescence and irradiation of $Ru(dpp(SO_3)_2)_3$ was repeated three or four times. The intensity of the light used to irradiate the $Ru(dpp(SO_3)_2)_3$ was 6.2×10^{-6} einstein dm^{-3} s^{-1}, as measured using a Coherent Fieldmaster power meter with model LM-2 semiconductor detector head (Coherent Inc., Santa Clara, CA, USA).

The leaching experiments were performed in an Amicon tangential filtration system, using Biomax 50 kDa membranes (Milipore). Typically, 10 ml of a 3 mg ml^{-1} suspension of PEBBLES in saline phosphate buffer were added to a 25 mm diameter Amicon and allowed to filter. The first 2 ml were collected but unused and the absorption/fluorescence of the following 3 ml of filtrate was measured. All the filtrate was then placed back in the Amicon. This process was repeated several times to follow the leaching and occasionally the total absorption/fluorescence of the suspension was measured to account for alterations in the total amount of dye.

3. Kinetic model

The production of $^1O_2$ by $Ru(dpp(SO_3)_2)_3$ and measurement by the reaction of $^1O_2$ with ADPA is described in

Ru	+	hν (465nm)	→	Ru*			I^{abs}
		Ru*	→	Ru	+	hν (620nm)	k_F
		Ru*	→	Ru			k_0
Ru*	+	$^3O_2$	→	Ru	+	$^1O_2$	k_1
ADPA	+	$^1O_2$	→	$ADPAO_2$			k_2
		$^1O_2$	→	$^3O_2$			k_3
		ADPA	→	Y			k_Y

Scheme 1. Kinetic scheme for production and measurement of $^1O_2$ under steady state irradiation.

Scheme 1. Ru represents $Ru(dpp(SO_3)_2)_3$ in the ground state, free in solution or entrapped inside the nanoparticles, that can be excited by 465 nm light, creating Ru^* with a rate constant equal to the intensity of light absorbed, I^{abs}, in units of einstein $dm^{-3}\ s^{-1}$. The excited molecule may decay to the ground state with the emission of a photon or non-radiatively with the rate constants k_F and k_0, respectively. Ru^* can also transfer energy to the ground state molecular oxygen, $^3O_2$, and excite it into singlet oxygen, $^1O_2$, while Ru^* decays to the ground state with the rate constant k_1. The $^1O_2$ formed may react with ADPA to form the endoperoxide $ADPAO_2$ with the rate constant k_2. The singlet oxygen molecule may also decay to the ground state by energy transfer to the solvent or other molecules in solution with a rate constant k_3, this process including also eventual reaction with molecules other than ADPA. In the kinetic scheme, the possibility is also considered of ADPA being consumed in processes not involving $^1O_2$ with a rate constant k_Y.

From kinetic Scheme 1, the following differential equations are obtained:

$$\begin{aligned}
\frac{d[Ru]}{dt} &= -I^{abs} + (k_0 + k_F + k_1[^3O_2])[Ru^*] \\
\frac{d[Ru^*]}{dt} &= I^{abs} - (k_0 + k_F + k_1[^3O_2])[Ru^*] \\
\frac{d[ADPA]}{dt} &= -(k_2[^1O_2] + k_Y)[ADPA] \\
\frac{d[^1O_2]}{dt} &= k_1[^3O_2][Ru^*] - \{k_3 + k_2[ADPA]\}[^1O_2]
\end{aligned} \tag{1}$$

The integration of Eq. (1) can be simplified if the rate of deactivation of $^1O_2$ by reaction with ADPA is negligible compared to the deactivation by the solvent, i.e. $k_3 \gg k_2[ADPA]$. In our particular case $k_3 \cong 3 \times 10^5\ s^{-1}$ [12], $k_2 \cong 1 \times 10^8\ M^{-1}\ s^{-1}$ [13] and $[ADPA] \cong 1 \times 10^{-5}$ M, therefore we are comparing 3×10^5 with 10^3. With this simplification the rate equation for $^1O_2$ is independent of [ADPA] and therefore unchanged over the irradiation time, and the decay of [ADPA] follows first-order kinetics, Eq. (2). The expressions for the quantum yield of $^1O_2$ production by $Ru(dpp(SO_3)_2)_3$ and for the concentrations $^1O_2$ under steady state irradiation are presented in Eqs. (3) and (4), respectively.

$$[ADPA] = [ADPA]_{t=0} \exp(-kt),$$

$$k = \frac{\Phi^{^1O_2} k_2 I^{abs}}{k_3} + k_Y \tag{2}$$

$$\Phi^{^1O_2} = \frac{k_1[^3O_2]}{k_0 + k_F + k_1[^3O_2]} \tag{3}$$

$$[^1O_2] = \frac{\Phi^{^1O_2} I^{abs}}{k_3} \tag{4}$$

For the production/measurement of $^1O_2$ in the presence of sodium azide, the reaction of $^1O_2$ with N_3^-, with a rate constant k_4, must be added to the kinetic scheme. The resulting differential equations may be integrated assuming the same conditions as before and the rate constant for the decrease of the concentration of ADPA with the irradiation time is now given by (5).

$$k = \frac{\Phi^{^1O_2} k_2 I^{abs}}{k_3 + k_4[N_3^-]} + k_Y \tag{5}$$

4. Results

The polyacrylamide particles were easily suspended in saline phosphate buffer producing a clear, non-turbid, suspension after sonication for 10–30 min. The measurement of the size of the nanoparticles was performed with multi-angle light scattering after separation of sizes by asymmetric field flow fractionation. The concentration of nanoparticles used was usually 10 mg ml^{-1} but a concentration of up to 300 mg ml^{-1} was tested to check for aggregation of the nanoparticles at higher concentrations. For the higher concentrations a smaller volume of sample was injected to avoid saturation of the light scattering detector. The results obtained are presented in Fig. 3. The preparations presented in Fig. 3A were prepared in different days and with a different amount of $Ru(dpp(SO_3)_2)_3$ per gram of

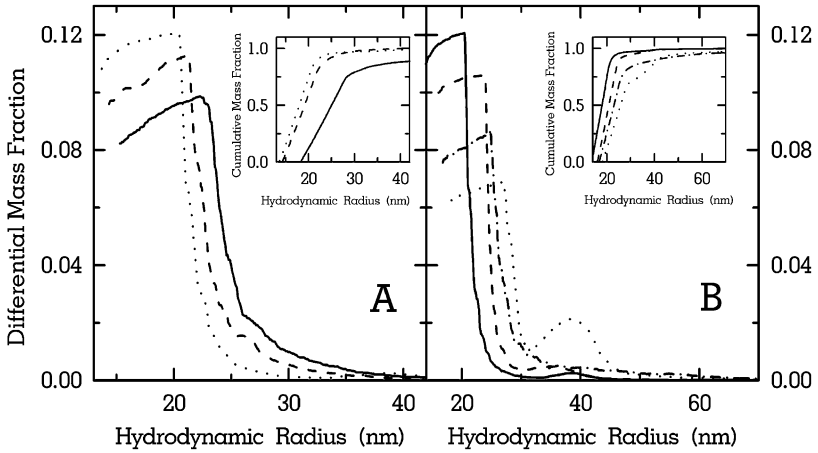

Fig. 3. Differential mass fraction as a function of the hydrodynamic radius of PAA nanoparticles suspended in saline phosphate buffer. Insert—cumulative mass fraction as a function of the hydrodynamic radius. (A) Different preparations of particles at a concentration of 10 mg ml^{-1} and with a different amount of $Ru(dpp(SO_3)_2)_3$ per gram of nanoparticles: 6 μmol g^{-1} (—), 16 μmol g^{-1} (- - -) and blank particles (· · ·). (B) Different concentrations of particles of the same preparation: 10 mg ml^{-1} (—), 33 mg ml^{-1} (- - -), 100 mg ml^{-1} (· · ·) and 300 mg ml^{-1} (- · -).

nanoparticles: 6 μmol g^{-1} (—), 16 μmol g^{-1} (- - -) and blank particles (· · ·). It can be seen that there is little variation with the preparation and with the loading of the particles with dye in this concentration range. The results presented in Fig. 3B were obtained with the same preparation of blank particles at several concentrations. The particles are easily suspended in saline phosphate buffer with a concentration up to 300 mg ml^{-1}. With the high concentrations some aggregation is observed but those aggregates may be broken up by sonication. In Fig. 3B, one can see that the solution with 100 mg ml^{-1} presented more aggregation than the solution with 300 mg ml^{-1} that was sonicated for a longer period. Even with the presence of some aggregation, more than 90% of the particles/aggregates presented a hydrodynamic radius smaller than 40 nm (see insert in Fig. 3).

The leaching of $Ru(dpp(SO_3)_2)_3$ from the nanoparticles was measured using an Amicon tangential filtration system, using Biomax 50 kDa membranes as described in the methods section. The samples were prepared in phosphate buffer 10 mM, pH 7, with 0.15 M NaCl, and were sonicated until clear, 10–30 min for PAA and 1–5 h for AFPAA. The results obtained in a typical experiment are presented in Fig. 4. The leaching from AFPAA nanoparticles is very small with less than 4% of free dye being detected, for a preparation of 1 mg ml^{-1} of nanoparticles with 6.2 μmol Ru g^{-1}, after 2 days in saline phosphate buffer (Fig. 4A). The leaching from PAA nanoparticles present a biphasic behavior with about 30% of the dye leaching out very fast and the remaining leaching out relatively slowly, about 10% in 1 day (Fig. 4B). The total amount of dye in the suspension is also presented in Fig. 4 and a small decrease was observed, this being attributed to binding of the free dye to the membrane.

The characterization of $Ru(dpp(SO_3)_2)_3$ as a source of $^1O_2$ in saline phosphate buffer equilibrated with air was performed by irradiation in a fluorimeter in the presence of 12 μM of ADPA (absorption = 0.1 at 380 nm). The ADPA

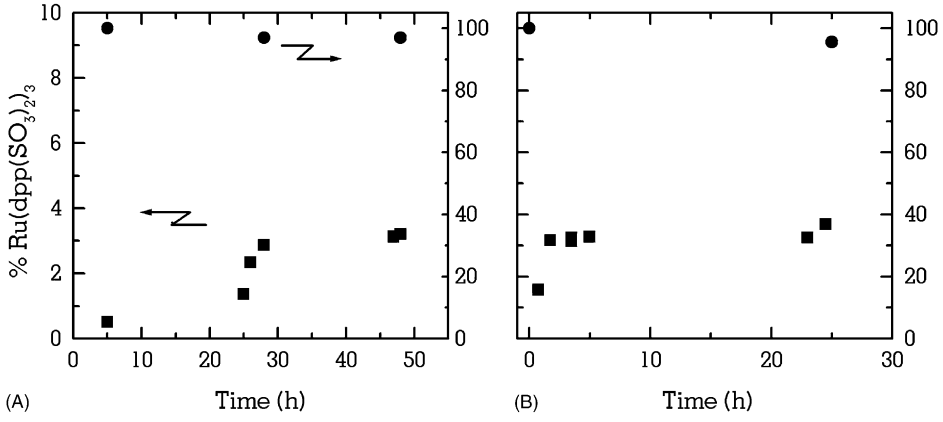

Fig. 4. Percentage of $Ru(dpp(SO_3)_2)_3$ that leached out of the nanoparticles (■) and total dye (●) as a function of time from the preparation of the solution in saline phosphate buffer, pH 7. (A) Data for AFPAA particles with 6 μmol of $Ru(dpp(SO_3)_2)_3$ per gram of nanoparticles. (B) Data for PAA particles with 16 μmol of $Ru(dpp(SO_3)_2)_3$ per gram of nanoparticles.

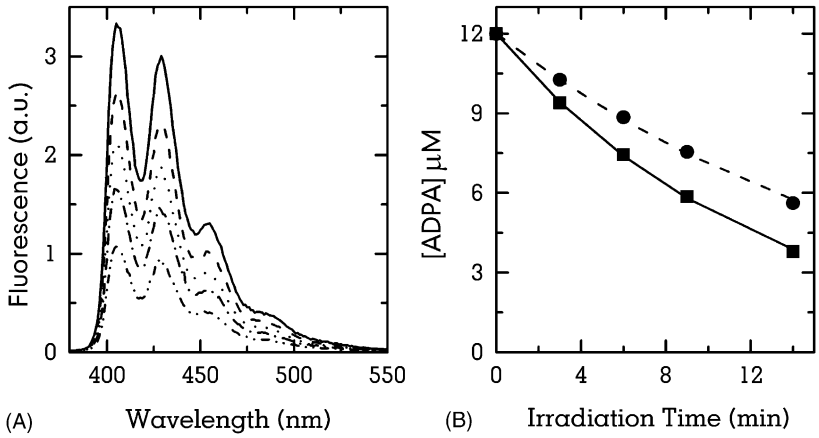

Fig. 5. Decrease of ADPA concentration by the irradiation at 465 nm of a solution containing ADPA and $Ru(dpp(SO_3)_2)_3$. (A) Fluorescence of ADPA when excited at 380 nm before irradiation (—), and after irradiation of 40 μM of $Ru(dpp(SO_3)_2)_3$ for 3 min (- - -), 6 min (· · ·), 9 min (- · -) and 14 min (- · · -). (B) Concentration of ADPA as a function of the time of irradiation of 40 μM (■) and 20 μM (●) $Ru(dpp(SO_3)_2)_3$. The best fit of Eq. (2) is also shown and the rate constants obtained are presented in Table 1.

reacts with $^1O_2$ to form an endoperoxide (Fig. 2) and the disappearance of ADPA can be followed by the decrease in fluorescence in the range 400–500 nm when excited at 380 nm. The results obtained for irradiation of a solution of 40 μM free $Ru(dpp(SO_3)_2)_3$, with a light intensity of 6.2×10^{-6} einstein $dm^{-3}\ s^{-1}$ at 465 nm, are presented in Fig. 5A. The concentration of ADPA can be calculated from the fluorescence intensity, assuming a linear dependence, and this is presented in Fig. 5B for the irradiation of a solution of $Ru(dpp(SO_3)_2)_3$ at 40 and 20 μM. The best fit of Eq. (2) to the experimental results is also shown and the values of k obtained are 1.3×10^{-3} and $8.8 \times 10^{-4}\ s^{-1}$ for $[Ru(dpp(SO_3)_2)_3] = 40$ and 20 μM, respectively. The ratio of the rate constants obtained for the different concentrations of $Ru(dpp(SO_3)_2)_3$ is in excellent agreement with the predictions from the kinetic model used.

The parameter that is more relevant to this work is the quantum yield of singlet oxygen production, $\Phi^{^1O_2}$. Before we can calculate $\Phi^{^1O_2}$ from Eq. (2) we need to measure the rate constant k_Y, and this was obtained by irradiation in the presence of different concentrations of NaN_3. The azide ion is an efficient quencher of $^1O_2$, $k_4 = 4.5 \times 10^8$ to $6.4 \times 10^8\ M^{-1}\ s^{-1}$ [12], and if the consumption of ADPA is only via $^1O_2$ the value recovered for k should approach 0 as the concentration of NaN_3 increases [14–16]. The results obtained for two different concentrations of $Ru(dpp(SO_3)_2)_3$ are presented in Fig. 6. From the best fit of Eq. (5) to the experimental results, the values $k_4 = 6.0 \times 10^8$ (4.2×10^8) $M^{-1}\ s^{-1}$, $k_Y = 3.1 \times 10^{-4}$ $(4.2 \times 10^{-4})\ s^{-1}$ and $\Phi^{^1O_2} = 0.86$ (0.76) are obtained for $[Ru(dpp(SO_3)_2)_3] = 20$ (40) μM. The rate constants used and recovered from the best fit of the kinetic model are collectively presented in Table 1 for all the samples tested.

The same methodology applied to characterize $Ru(dpp(SO_3)_2)_3$ free in solution was applied to the dye incorporated in PAA and AFPAA particles. The results obtained in a typical experiment are presented in Fig. 7. The results for two different concentrations PAA nanoparticles with 16 μM $Ru(dpp(SO_3)_2)_3$ per gram of nanoparticle are presented in Fig. 7A. The time profile was very well described by the kinetic model and the values obtained for k indicate that the polyacrylamide matrix does not quench the $^1O_2$ formed inside them allowing it to leave the nanoparticles and react with the ADPA dissolved in the solution. The suspension of the AFPAA nanoparticles in saline phosphate buffer is much more difficult than in the case of PAA particles and they must be sonicated for hours before a clear solution is obtained. The results obtained with the clear solution, after sonication for 5 h, and with a sample of the same suspension sonicated for only 1 h are presented in Fig. 7B. The solution sonicated for only 1 h presented some scatter at the wavelength used for irradiation, the apparent absorption at 465 nm was 1.9 while the absorption by $Ru(dpp(SO_3)_2)_3$ after the aggregates have been broken is only 0.25. It is observed that the presence of scatter increases the rate of production of $^1O_2$ and this was

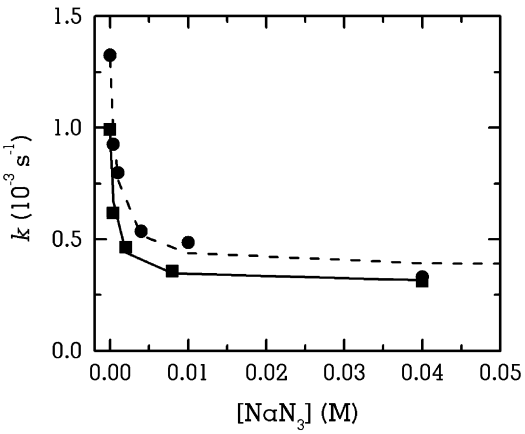

Fig. 6. Dependence of the rate constant for disappearance of ADPA, k, as a function of the concentration of NaN_3 for a concentration of $Ru(dpp(SO_3)_2)_3$ of 40 μM (■) and 20 μM (●). The best fit of Eq. (5) is also shown and the rate constants obtained are presented in Table 1.

Table 1
Rate constants recovered from the best fit of the kinetic model to the production of $^1O_2$ by $Ru(dpp(SO_3)_2)_3$ in saline phosphate solution, free and incorporated in PAA and AFPAA nanoparticles

Matrix	[Nanoparticles] (g ml^{-1})	[$Ru(dpp(SO_3)_2)_3$] (μM)	k (s^{-1})/(I^{abs}/I^0)	$\Phi^{1}O_2$
None	–	20–50	2.3 (±0.1) × 10^{-3}	0.80 ± 0.05
PAA	1–5	10–50	2.6 (±0.2) × 10^{-3}	
AFPAA	1–2	6–30	1.4 (±0.3) × 10^{-3}	

The concentration of ADPA was always 12 μM and I^0 (465 nm) = 6.2 × 10^{-6} einstein dm^{-3} s^{-1}, the values used from the literature for the other rate constants were ε_{Ru} (465 nm) = 10^4 M^{-1} cm^{-1} [20], ε_{ADPA} (400 nm) = 8.5 × 10^3 M^{-1} cm^{-1} [21], k_2 = 1 × 10^8 M^{-1} cm^{-1} [13], k_3 = 3 × 10^5 s^{-1} [12], and k_4 = 5.5 (±1.0) × 10^8 M^{-1} cm^{-1} [12].

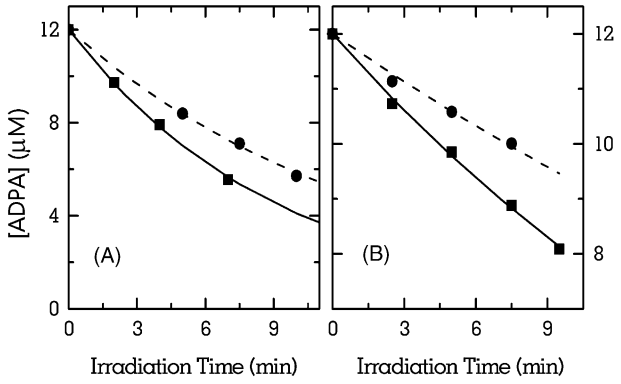

Fig. 7. (A) Decrease in the concentration of ADPA due to irradiation of $Ru(dpp(SO_3)_2)_3$ entrapped in PAA nanoparticles with a concentration of 47 μM (■) or 24 μM (●) relative to the total volume. (B) Decrease in the concentration of ADPA due to irradiation of $Ru(dpp(SO_3)_2)_3$ entrapped in AFPAA nanoparticles with a concentration of 16 μM relative to the total volume, after sonication for 1 h (■) or 5 h (●).

interpreted as being due to an increase in the effective pathlength of the excitation light. After sonication the samples were allowed to equilibrate with air before the commencement of the kinetic experiment and the values recovered for the rate constants in the clear solutions show that when $Ru(dpp(SO_3)_2)_3$ is incorporated in AFPAA particles the rate of consumption of ADPA is reduced to about 60% as compared to the experiments with free $Ru(dpp(SO_3)_2)_3$. The rate constants used and recovered from the best fit of the kinetic model are collectively presented in Table 1.

5. Discussion

The size of the amine-functionalized nanoparticles have not been directly measured because the membranes used in the asymmetric field flow fractionation equipment are not compatible with amines. It is expected that the sizes are similar because the micro-emulsion used for the polymerization has the same characteristics. Also, the size of AFPAA particles prepared by the same method have been measured indirectly after reaction of the amine groups with polyethylene glycol 2000 (PEG2000). Those PEG modified AFPAA particles possess a hydrodynamic radius of about 40 nm.

A bulk gel prepared with the acrylamide concentration used in the preparation of the nanoparticles (21% acrylamide and 6% bis-acrylamide) is an efficient sieve for molecules with a molecular weight higher than 2 kDa [17]. It was therefore expected that the particles prepared, both PAA and AFPAA, would efficiently entrap the 2.7 kDa $Ru(dpp(SO_3)_2)_3$. The results obtained with the PAA particles show that although the core of the particles is an efficient sieve, the interface of the particles is more leaky and, as expected, the interface of a particle with r = 25 nm represents a significant fraction of the total volume. The results obtained with AFPAA indicate that the interaction between the negatively charged dye (−6) and the ionized amine groups in the particles is strong enough to slow down the kinetics of leaching so that the dye does not leach significantly during a period of days. The PAA particles may be washed with saline buffer and the $Ru(dpp(SO_3)_2)_3$ remaining in the particles will not leach out significantly during several hours.

The kinetic model used assumes a random distribution of all the reactants, $Ru(dpp(SO_3)_2)_3$, $Ru(dpp(SO_3)_2)_3^*$, $^3O_2$, $^1O_2$ and ADPA and the good fit of the model to the experimental results does not make us suspect of heterogeneities. We have also observed that the absorption and fluorescence spectra of $Ru(dpp(SO_3)_2)_3$ and ADPA are not affected by one another and also that ADPA are not affected by the presence of PAA or AFPAA nanoparticles. In contrast, the fluorescence emission spectra of $Ru(dpp(SO_3)_2)_3$ incorporated in the particles is blue shifted by 5 and 10 nm in PAA or AFPAA, respectively (results not shown). However, there are several possible heterogeneities that should be taken into account in the interpretation of the results: (i) in the case of free $Ru(dpp(SO_3)_2)_3$ the only concern is that both $Ru(dpp(SO_3)_2)_3$ and ADPA are negatively charged, −6 and −2, respectively. This however should not lead to a significant repulsion between the two molecules due to the high ionic strength of the media, I = 0.165 M. (ii) The number of molecules of $Ru(dpp(SO_3)_2)_3$ per nanoparticle in the preparations used ranged from some about 10–100 and the distribution of $Ru(dpp(SO_3)_2)_3$ relative to the total volume is obviously not homogeneous. This does not present a problem due to the low intensity of irradiation light, where the probability of excitation of two molecules in the same particle is negligible, and therefore conducing to a random distribution of $Ru(dpp(SO_3)_2)_3$ in the excited state. (iii)

ADPA ($M_W = 366$ g mol^{-1}) is small enough to freely enter the nanoparticles and its concentration inside the nanoparticles is mainly determined by the relative solubility in the two media. The concentration of ADPA inside/close to the AFPAA nanoparticles may be higher due to electrostatic interaction with the positively charged particles. (iv) The concentration of $^3O_2$ and $^1O_2$ inside the particles is only determined by the relative solubility in the two media.

The inclusion in the kinetic scheme of a reaction for the consumption of ADPA not mediated by $^1O_2$ was done previously by other authors that have noticed a discrepancy between the results obtained with ADPA and other methods of detection of $^1O_2$ [18]. Without this step our results for the consumption of ADPA indicated an apparent $\Phi^{^1O_2} = 1.12 \pm 0.06$ for $Ru(dpp(SO_3)_2)_3$ free in solution. This excessively high quantum yield of $^1O_2$ production is consistent with the literature value of $\Phi^{^1O_2} = 1.0 \pm 0.1$ for $Ru(bpy)_3$ also measured with ADPA and neglecting the non-$^1O_2$ mediated step [13]. The value obtained with the complete kinetic scheme, $\Phi^{^1O_2} = 0.80 \pm 0.05$, is similar to the values found for other Ruthenium complexes using direct methods [19].

The values obtained for the rate of consumption of ADPA when $Ru(dpp(SO_3)_2)_3$ is inserted in the nanoparticles as compared to the free dye cannot be directly translated into differences in $\Phi^{^1O_2}$ because the matrix may affect k in several ways that were not evaluated, namely (i) the matrix may increase the local concentration of $^3O_2$, (ii) the matrix may quench the $^1O_2$ produced, and (iii) the matrix may affect k_Y. From the above effects only (iii) is important because the parameter relevant for applications of the nanoparticles in PDT is the amount of $^1O_2$ produced. This non-$^1O_2$ mediated consumption of ADPA has been interpreted as energy transfer from the sensitizer to ADPA to form ADPA in the triplet excited state, $^3ADPA^*$, followed by reaction of $^3ADPA^*$ with $^3O_2$ to form an endoperoxide [18]. The value of k_Y in the presence of the nanoparticles was not measured but the inclusion of $Ru(dpp(SO_3)_2)_3$ in the nanoparticles should inhibit this step due to the physical separation of the two molecules. Therefore, the comparison of k obtained for the free dye and with PAA nanoparticles does indicate a higher production of $^1O_2$ by $Ru(dpp(SO_3)_2)_3$ incorporated in those particles. The results obtained with the AFPAA matrix indicate a decrease in the release of $^1O_2$ to the aqueous media because the observed decrease in k cannot be attributed only to a decrease in k_Y.

6. Conclusions

The quantum yield of singlet oxygen production by $Ru(dpp(SO_3)_2)_3$ in saline phosphate buffer equilibrated with air has been measured, $\Phi^{^1O_2} = 0.80 \pm 0.05$.

Nanoparticles with a polyacrylamide matrix and a hydrodynamic radius of 20–25 nm have been produced that efficiently entrap $Ru(dpp(SO_3)_2)_3$ and do not quench the $^1O_2$ produced. Nanoparticles with an amine-functionalized polyacrylamide matrix have also been prepared and they present a very slow leaching of $Ru(dpp(SO_3)_2)_3$. Those AFPAA particles reduce the amount of $^1O_2$ detected by ADPA to about 60% as compared with the free dye but they are still useful as sources of $^1O_2$. The amine groups on the surface of the particles may be reacted with molecules for purposes of both cloaking (e.g. PEG) and targeting moieties for tumor-specific molecular receptors. Systemic delivery of these modified particles would enable tumor-specific localization of these nanoparticles within the tumor mass. It is envisioned that photodynamic activation would be achievable which would result in the local production of $^1O_2$ for providing a significant therapeutic benefit.

We are currently working on the development of nanoparticles with an $^1O_2$ sensor molecule enclosed, with the purpose of measuring the amount of $^1O_2$ produced in situ. The work presented in this paper shows that the PAA matrix does not quench significantly the $^1O_2$ and therefore those nanoparticles may be used for the development of $^1O_2$ sensors.

Acknowledgements

The research described was financed by NCI, contract number N01-CO-07013. Maria J. Moreno is indebted to FCT-Portugal for a Grant SFRH/BPD/1593/2000.

References

[1] I.J. MacDonald, T.J. Dougherty, Basic principles of photodynamic therapy, J. Porphyr. Pthalocya. 5 (2001) 105–129.
[2] H.A. Clark, M. Hoyer, M.A. Philbert, R. Kopelman, Optical nanosensors for chemical analysis inside single living cells. 1. fabrication, characterization, and methods for intracellular delivery of PEBBLE sensors, Anal. Chem. 71 (1999) 4831–4836.
[3] A.K. Gupta, S. Madan, D.K. Majumdar, A. Maitra, Ketorolac entrapped in polymeric micelles: preparation, Int. J. Pharm. 209 (2000) 1–14.
[4] M. Philbert, et al., unpublished results.
[5] V. Nardello, J.M. Aubry, Methods Enzymol. 319 (2000) 50–58.
[6] N.J. Turro, M.F. Chow, J. Rigaudy, Mechanism of thermolysis of endoperoxides of aromatic-compounds–activation parameters, magnetic-field, and magnetic isotope effects, J. Am. Chem. Soc. 103 (1981) 7218–7224.
[7] W. Drews, R. Schmidt, H.D. Brauer, Photolysis of the endoperoxide of 9,10-diphenylanthracene, Chem. Phys. Lett. 70 (1980) 84–88.
[8] J. Rigaudy, C. Breliere, P. Scribe, Photochemistry of 9,10-diphenylanthracene endoperoxide, Tetrahedron Lett. (1978) 687–690.
[9] B.A. Lindig, M.A.J. Rodgers, A.P. Schaap, Determination of the lifetime of singlet oxygen in D_2O using 9,10-anthracenedipropionic acid, a water-soluble probe, J. Am. Chem. Soc. 102 (1980) 5590–5593.
[10] B.A. Lindig, M.A.J. Rodgers, Rate parameters for the quenching of singlet oxygen by water-soluble and lipid-soluble substrates in aqueous and micellar systems, Photochem. Photobiol. 33 (1981) 627–634.
[11] F.N. Castellano, J.R. Lakowicz, A water-soluble luminescence oxygen sensor, Photochem. Photobiol. 67 (1998) 179–183.
[12] http://www.rcdc.nd.edu/index.html.
[13] K.O. Zahir, A. Haim, Yields of singlet dioxygen produced by the reaction between the excited-state of tris(bipyridine)ruthenium(II)

and triplet dioxygen in various solvents, J. Photochem. Photobiol. A: Chem. 63 (1992) 167–172.
[14] R.D. Hall, C.F. Chignell, Steady-state near-infrared detection of singlet molecular-oxygen—Stern–Volmer quenching experiment with sodium-azide, Photochem. Photobiol. 45 (1987) 459–464.
[15] W.R. Haag, T. Mill, Rate constants for interaction of o-1(2) (1-delta-g) with azide ion in water, Photochem. Photobiol. 45 (1987) 317–321.
[16] A. Seret, E. Gandin, A. Vandevorst, Singlet oxygen production by UV and visible photoexcited porphyrins under different states of aggregation, Photobiochem. Photobiophys. 12 (1986) 259–266.
[17] B.D. Hames, D. Rickwood, Gel Electrophoresis of Proteins, A Practical Approach, IRL Press, Washington, DC, USA, 1981.
[18] E. Gandin, Y. Lion, A. Vandevorst, Quantum yield of singlet oxygen production by xanthene derivatives, Photochem. Photobiol. 37 (1983) 271–278.
[19] J.N. Demas, E.W. Harris, R.P. Mcbride, Energy-transfer from luminescent transition-metal complexes to oxygen, J. Am. Chem. Soc. 99 (1977) 3547–3551.
[20] S. Anderson, E.C. Constable, K.R. Seddon, J.E. Turp, J.E. Baggott, M.J. Pilling, Preparation and characterization of 2,2′-bipyridine-4,4′-disulphonic and bipyridine-5-sulfonic acids and their ruthenium(II) complexes—excited-state properties and excited-state electron-transfer reactions of ruthenium(II) complexes containing 2,2′-bipyridine-4,4′-disulphonic acid or 2,2′-bipyridine-4,4′-dicarboxylic acid, J. Chem. Soc., Dalton Trans. (1985) 2247–2261.
[21] http://www.probes.com.